TD-03-012

Superconducting RF Material R&D at Fermilab

PROPOSAL

Pierre Bauer
Fermilab, Technical Division
April 2003

The following proposal for a combined material science and superconducting RF research project will allow Fermilab to participate in the worldwide quest for cost reduction and performance improvement of superconducting RF technology. At the heart of this proposal lies a so-called small sample test facility, which allows measuring the breakdown magnetic fields of small, cm^2 sized samples under high power RF. In combination with state of the art surface analysis tools, the small sample tests become a powerful tool to investigate surface and material issues related to very high power RF. The small sample test allows predicting the theoretical limits of the cavity performance and therefore to discriminate between material and cavity production related issues. It can therefore strongly benefit any superconducting RF cavity development, such as for example for Fermilab's CKM project or a possible superconducting proton driver linac. This tool can also be used to investigate other RF materials such as Nb_3Sn with the potential to exceed the gradients achievable in sheet Niobium cavities. These advanced superconducting RF material options have the potential to reduce cost and increase operating gradient of superconducting linacs in the future, such as for example for a future linear electron-positron collider. The project is envisioned to unfold within the Technical Division at Fermilab.

Table of Contents

Acknowledgment

This proposal includes suggestions and ideas from the following persons:

H. Edwards, R. Kephart, D. Finley, N. Solyak, T. Khabiboulline, L. Bellantoni, G. Romanov, C. Bohn, G.W. Foster, V. Yarba, W. Fowler, T. Nicol, T. Peterson (FNAL), H. Padamsee (CU), D. Proch, W. Singer, R. Wanzenberg (DESY), R. Scanlan (LBNL), S. Calatroni, E. Mahner, E. Chiaveri (CERN), M. Peiniger (ACCEL), A.M. Valente, P. Kneisel (TJNAF) and D. Larbalestier, A. Gurevich, P. Lee (UW).

I am very indebted to all of them for their contributions!

1. Proposal Summary

The following proposal is addressing the need for RF material characterization and development in the context of several projects at Fermilab, that make use of superconducting high gradient RF cavity technology. A novel approach. consisting of the measurement of the performance limits of small samples of superconducting RF materials, will allow to discriminate between performance limitations brought about in superconducting cavities by production steps or by the intrinsic limitation of the material or its particular surface composition. It consists of placing a small, several cm^2 sized, cylindrical sample into the axis of a high performance, single cell TESLA type cavity in a TE010 mode (2.5 GHz). With the right choice of operating parameters a surface magnetic field enhancement by a factor of 2-3 can be achieved, such as to allow the measurement of materials exceeding the performance limit of state of the art Niobium. Together with existing surface analysis tools, such as scanning electron microscopy and Auger spectroscopy, this small sample facility can become a very powerful tool to investigate established and yet un- (or not sufficiently) explored alternate superconducting RF materials.

The fundamental issues in superconducting RF technology are cost and maximum gradient. A possible route to significant cost savings in superconducting cavities is to replace the bulk Niobium with Niobium on Copper. Explosion bonding and hot extrusion were recently proposed as new approaches to produce Niobium-Copper composite cavities. Materials such as Nb_3Sn and NbN could, if exploited to their full potential, yield a factor 2 increase in accelerating gradient with respect to Niobium. Alternatively the advantage offered by these materials could also be translated into reduced operations cost if the choice is made to keep the same gradient but operate at increased Q and/or operate at higher temperature (such as 4.2 K). An approach worth exploring is the coating of state of the art, single-cell, bulk Niobium cavities with Nb_3Sn (or NbN).

As a first step we propose to engage in a material research study to explore the surface issues and quench fields of small samples of state of the art Niobium. This part of the program will be an important asset for existing superconducting cavity development programs at Fermilab, for example related to CKM, [1], and possible future projects such as a superconducting proton driver linac, [2]. It is imagined that small witness samples that accompany superconducting cavities throughout production can then be measured in this facility to evaluate the surface quality obtained and to study effects due to the many production steps. In the future the activity could be expanded toward the exploration of other materials, such as mentioned above. The unique experimental approach proposed here will allow exploration, with unprecedented reach, of the fundamental physics of RF superconductivity. This has repeatedly been listed as a high priority task by the superconducting RF community (see for example items 99 and 101-103 in the linear collider related R&D task list, [3]).

This project should unfold within the Technical Division at Fermilab. A possible collaboration with the University of Wisconsin, where state of the art surface analysis tools exist, was discussed. The university group can contribute in a significant way through its expertise and equipment in surface and superconducting material science as well as with its expertise in superconducting RF theory. The project goals are discussed together with a rough outline of the FY03 budget in chapter 5. Chapter 2 reviews the main issues in the field of superconducting RF today and shows how this proposal addresses some of them. In addition, an attempt was made to review the experimental

techniques used at other labs in support of superconducting cavity development (chapter 4). We also review past experience with materials other than niobium in the quest for high gradients (chapter 3).

2. Current Issues in Superconducting RF Technology

2.1 Introduction

Following the pioneering development of superconducting cavities built from lead at SLAC, [4,5], the research in superconducting materials for RF applications today has focused on pushing Niobium to its theoretical limit. Recent, dramatic advances in the context of the linear collider R&D were made possible through the concerted efforts of the DESY, Cornell, TJNAF, KEK, CEA, INFN (Genova, Legnaro, Milano), University of Wuppertal, ANL laboratories and other institutions and companies (ACCEL). Industrially produced, Niobium based multi-cell cavities now operate reliably at surface electric / magnetic fields of ~50 MVm^{-1} / ~120 mT (which corresponds to ~25 MV/m of accelerating gradient). Procedures such as high power processing, BCP etching and/or electro-polishing, quality requirements for the raw material (min RRR and max defect size) and optimized processing technologies (such as post-purification with titanium getter) are key elements of this success. As outlined in the TESLA design report, [6], the superconducting linear collider can now reach 500 GeV in the center of mass within a ~30 km site. The current TESLA upgrade path consists of achieving 800 GeV in the center of mass within the same tunnel with a 35 MV/m accelerating gradient. This gradient is believed to be close to the maximum that can be obtained in mass-produced cavities made from sheet Niobium. Ideally, even higher energies are desirable. Unfortunately the wall-loss and operations cost increase with gradient as well. Also, detrimental effects such as field emission (which is now suppressed for the 25 MV/m accelerating gradient range through improved cleanliness) will most likely re-emerge. Reaching limiting gradients will also challenge once again the theory of superconducting RF limitations, [7].

We believe that the most important issues that the field of superconducting RF currently faces are -1- cost savings in view of the unprecedented scale of more than 20000 cavities for a linear collider such as TESLA and -2- higher gradients in view of a TESLA upgrade or smaller scale superconducting RF projects such as the Fermilab proton driver. The following proposal addresses these issues and will allow Fermilab to make an impact in the quest for better and cheaper superconducting cavities. The following chapter discusses the rationale for the proposed superconducting RF material R&D. It encompasses a cost analysis of state of the art cavities for TESLA, a discussion of the impact of gradient, Q and operating temperature on the cost and operation of a TESLA type collider as well as the effects limiting the performance of cavities. The discussion in this chapter presents the rationale for the proposed superconducting RF material R&D.

2.2 The Cost of Superconducting Cavities

A recent review of the TESLA cavity cost-estimate, [8], contains the following cavity cost break-down (Table 1). As of today, the cost per m of cavity (including cryostat) is ~100 k$. A factor 2 cost saving is projected in view of a mass production for TESLA.

Table 1: 2002 TESLA bulk niobium cavity cost for the Tesla Test Facility (from reference [8]).

component	sub-component	cost/m (k$)	comment
naked cavity		*50*	
	material	*16.5*	RRR=300 grade niobium at 400 $/kg
	e-beam welding	*16.5*	strong reduction expected in mass production
	machining cups	*12*	cost of deep drawing is negligible
	HOM damper	*5*	2 per cavity
input coupler		*30*	each cavity is powered by its own coupler
tuner		*5*	Piezo actuator
magnetic shield		*5*	
cryo vessel		*5*	Titanium-alloy
miscellaneous		*5*	i.e. assembly man-power, cryostat welding
sum		**100**	

The cost reduction will be achieved through reduced machining and welding cost, reduced coupler cost using the so-called superstructure (one coupler per two cavities) as well as reduced material cost through recycling and economy of scale. The cost-estimate does not include testing. The projected TESLA cost of 50 k$/m has to be compared to 206 k$ per m of linac module in CEBAF, 377 k$ per m of linac module for SNS. The lower cost of TESLA is explained by a higher linac filling factor (0.35 in CEBAF, 0.45 in SNS vs. 0.7 in TESLA) and economy of scale (1716 TESLA cryo-modules vs. 43 cryo-modules at CEBAF). In addition, the size of the SNS cavities is much larger (800 MHz) and CEBAF cavities carry more bulky input and HOM couplers made from Nb. It is well known that cost savings can be generated by replacing Nb by Cu (at a cost of 8 $/kg instead of 400 $/kg, [9]) thereby reducing the cavity material cost from the projected ~8 k$/m (which assumes a factor 2 cost savings as compared to the number in the table in view of mass-production) to, in the best case, ~1 k$/m. Replacing the bulk Niobium entirely with Copper can deliver an extrapolated cost-savings of the order of 100 M$ in the production of the 21000 cavities for TESLA. Another cost-saving option, which is also being pursued by the TESLA collaboration, is the investigation of seamless cavity production techniques to reduce welding cost.

2.3 The Impact of Higher Gradient on the Design of a SC Linac

The impact of a higher cavity gradient on the overall cost of a superconducting linac can be studied on the basis of a simple model (such as discussed in [10]), weighting accelerator module and operating cost against tunneling cost. The result of such a calculation is presented in Figure 1. The exact formalism is described in detail in appendix A. The cavity cost is assumed to depend linearly on gradient, the slope being such that it intersects the $ 50k/cavity projected for TESLA at the 23.4 MV/m operating gradient (see discussion above). The operating cost is calculated from the static and RF-related loss and the Carnot efficiency to translate the cooling power requirement from low temperature to the plug. The tunneling cost recently quoted for the 3.66 m diameter tunnel for a VLHC is $ 9 M/km, which is believed to be at the low end of the

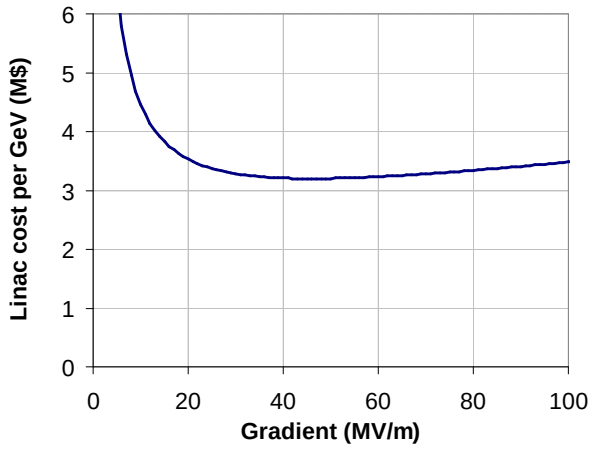

Figure 1: Calculated cost of linac (cavities, tunnel) and cryo-operations (over 10 years) for 1 GeV of acceleration. The calculation assumes a cavity cost of $ 1.9 k/(MV) (and an offset C_{cav0} of $ 5 k/m at zero gradient). The cryo-loss per unit length is given by the RF loss in the cavity walls (10^{13} Ω/m shunt impedance, 0.65% duty factor, fiddle factor FF was assumed to be 5 to account for the fact that the RF wall loss is only a fraction of the total dynamic RF loss in the cavity), the static heat load (300 W/m at the plug), the Carnot factor at 2 K (497). Ten operational years were assumed and the operational cost factor used is $1/W/(operational year). The calculation is discussed in detail in appendix A.

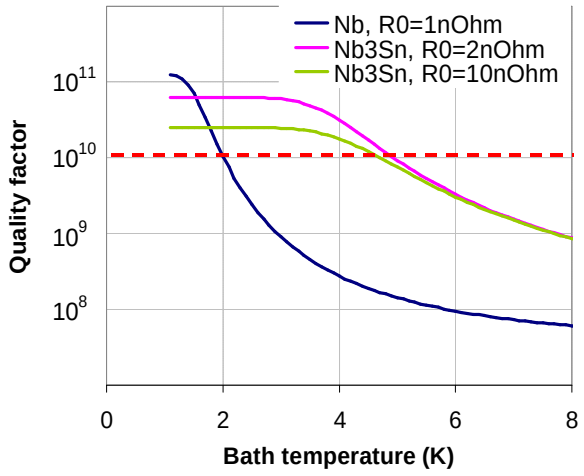

Figure 2: Calculated cavity quality factor for TESLA type cavities with 23.5 MV/m gradient and 1.3 GHz operating frequency for Niobium and Nb_3Sn surfaces (with residual surface resistance 1 nΩ in Nb and 2 and 10 nΩ in Nb_3Sn). The calculation is discussed in detail in appendix B.

tunneling cost spectrum. Linac tunnels with klystron galleries, such as for SNS, did cost ten times more. The number of accelerating structures (including the overhead factor 1.2) drops linearly with gradient, such that the linac cost runs through a broad minimum, diverging at very low gradient due to the large number of structures and tunneling cost and at high gradient due to the higher cost per structure and operations. The calculation leading to Figure 1 assumes parameters that are given in detail in the figure caption. Some of these parameters are typical for TESLA type cavities.

Figure 1 shows that the cost of a linac can be reduced at increased gradient up to ~40 MV/m. This trend would be even more pronounced if a higher tunnel cost is assumed. This conjecture, however, is strongly contingent on the assumption, that the cavity cost is linear (or less than linear) with gradient. Different assumptions can strongly affect the optimization shown in Figure 1. A more than linear increase of cost with gradient would result in an increase of the collider cost at larger gradients. Other cost-drivers, such as couplers and HOM-dampers, have not been factored into the calculation leading to Figure 1. Also not taken into account is the increase in Lorentz-force detuning at higher gradients (which in TESLA type cavities is 1 Hz/(MV/m)^2, [11]).

There is, however, another way to benefit from advances in superconducting RF cavities and materials. The BCS surface resistance drops exponentially with the critical temperature, T_c. Therefore, in principle, higher T_c materials such as Nb_3Sn, should lead to a higher quality factor, Q, and/or allow operation in boiling LHe at 4.5 K. An increased Q would benefit a linear collider, even at the same gradient, via savings in both the cryo-infrastructure and operating cost. Figure 2 shows Q as a function of bath temperature for Niobium and Nb_3Sn

calculated from the surface resistance (see appendix B for details). The surface resistance depends on the residual surface resistance and the BCS resistance, which in turn depends on the RF frequency (here 1.3 GHz), the bath temperature and the gap parameter *a* (a=17.7 K for Nb and 39.6 K for Nb_3Sn). The residual surface resistance in Niobium was assumed to be 1 nΩ and 2 and 10 nΩ in Nb3Sn. The plot in Figure 2 shows that, in the temperature range of interest, the lower BCS resistance in Nb_3Sn is mostly offset by the larger residual resistance. The net result, however, is that Nb_3Sn has a lower surface resistance than Niobium in the 2-5 K range, therefore being suited for 4.2 K operation at the same *Q* as Nb at ~2 K. Not easy to see in Figure 2 is that the Nb_3Sn surface resistance and thus the *Q*-factor drops by a factor ~2 between 2 and 4 K, therefore offsetting the factor ~2 gain in Carnot factor from 2 to 4 K, such that the site power for Nb_3Sn cavities is approximately flat in this temperature range. The models used here do not assume any drop of *Q* with gradient. In fact, as will be shown in chapter 3, experiments with Nb_3Sn have yet not produced such results.

2.4 Critical RF Fields

Experiments using pulsed mode cavity excitation, presented in [12,55], are at the basis of the theoretical understanding of the critical fields in type-I and type-II BCS superconductors. These experiments indicated that the maximum RF field to which superconductivity can be sustained is the so called superheating field, H_{sh}, given here as function of the Ginzburg-Landau parameter, k_{GL}, and the thermodynamic critical field, H_c. In type I (or very clean type II) superconductors where $k<1$, fields larger than the thermodynamic critical field can be reached. This is believed to be related to the nature of the vortex nucleation mechanism, which induces quenching in high frequency fields. The vortex nucleation times (several nsec) are of the same order or longer than the periods of microwave radiation and vortex penetration into the material is therefore lagging behind the excitation field, such that the quenching occurs at a field that is higher than the DC critical field. This model was verified in Niobium, but it still lacks verification in Nb_3Sn. Measurements are currently under way, [13,14], of the DC critical fields (H_{c1}, H_c and H_{c2}) in superconducting RF materials, as part of a renewed interest in the theoretical limiting fields. The correlation between the DC critical fields and RF critical fields is subject to discussion. In view of the current effort to push sheet Niobium cavities to the ultimate limit, it would be of interest to measure the critical fields in high power RF conditions. Formerly most cavities of the TESLA type, however, quenched as a result of defect heating or field emission. Improved surface preparation has pushed field emission onset higher, such that today single cell cavities fail mostly due to high field quenches, [6], and it is hoped that renewed efforts aiming at experimental evidence regarding the maximum quench fields might be successful this time.

$$H_{sh} = \begin{cases} \sim \dfrac{0.89}{\sqrt{k_{GL}}} H_c & k \ll 1 \\ \sim 1.2 H_c & k \sim 1 \\ \sim 0.75 H_c & k \gg 1 \end{cases} \quad \left(\frac{A}{m}\right)$$

3. Alternate Materials to Bulk Niobium

3.1 Overview of Superconducting RF Materials

The ideal (surface) material for superconducting RF applications exhibits a high critical field and temperature, a high thermal conductivity and a low surface resistance.

Unfortunately some of these requirements are conflicting and a compromise has to be found. Table 2 summarizes the parameters relevant for RF applications of known superconductors. To date, most superconducting cavities for accelerators are made of sheet Niobium or Niobium coated copper. Other superconductors, although superior in critical field and temperature (such as Nb_3Sn and NbN), have not yet been fabricated with the low levels of surface resistance at the high gradients required for a high gradient application. According to the current understanding there are three major contributions to surface resistance, [15]: the residual resistance R_0 (which can be related to normal conducting inclusions, surface oxides, interface and dielectric RF losses), the so-called BCS term (due to the unpaired electrons at the Fermi level), a possible flux-flow resistance term due to trapped flux R_{flux} and a term regrouping poorly understood contributions (called "non-quadratic losses" R_{nquad}), causing the so-called Q-slope.

$$R_s = R_0 + A\frac{l_L^3 w^2}{T_b} e^{-\frac{\Delta(0)}{k_B T_b}} + R_{flux}(H_{RF}, H_{ext}, T) + ... + R_{nquad}(H_{RF}, ...?) \quad (\Omega)$$

residual BCS trapped magnetic field unknown

As can be seen in the formula above, the BCS surface resistance term is characterized by a strong dependence on the London penetration depth and an exponential dependence on $1/T_c$ (via the gap energy $\Delta(0)$). In Nb_3Sn, for example, the BCS surface resistance term is expected to be smaller than in Niobium as a result of the higher T_c despite the two times larger London penetration depth. Indeed, Nb_3Sn is the most successful compound explored to date. Unfortunately, in the Nb_3Sn cavity prototypes produced so far with vapor diffusion of Tin on bulk Niobium cavities, the residual and non-quadratic resistance terms have dominated the surface resistance to a point where the performance was degraded with respect to bulk-Nb at gradients above 15 MV/m. The short coherence length of Nb_3Sn together with the granularity of the films produced is believed to be the cause of the large and non-quadratic residual resistance because of the larger sensitivity to small size defects and grain-boundaries. Other materials tested, also with limited success, are NbN and high temperature superconductors such as YBCO. The following briefly reviews the state of the art.

Table 2: Fundamental properties relevant for RF applications of known superconductors. All superconductors in the table are type II.

	critical temperature T_c (K)	thermodynamic critical field $\mu_0 H_{cth}$ (T)	experimentally achieved field $\mu_0 H$ (T)	coherence length? ξ_0 (nm)	penetration depth $\lambda_L(0)$ (nm)
Pb	7.2	0.08	0.12	83	48
Nb	9.2	0.2	0.23	60	40
Nb_3Sn	18	0.535	0.089	6	100
NbN_δ	16.2	~0.5	1	113	85
YBaCuO	93	1-1.4	0.75 -1.05	2/0.4	140 / 770

3.2 Niobium on Copper

The attractiveness of the composite route lies in the fact that the expensive RF material is reduced to a thin superconducting coating on a thicker, high thermal conductivity substrate that provides adiabatic and mechanical stabilization reducing cost at the same time. Copper has a superior thermal conductivity of 300-2000 W/m/K (vs. 75 W/m/K in RRR=300 Nb) and costs 50 times less and is therefore an ideal substrate material. CERN, for example, decided to use Niobium sputtered copper cavities for the LEP (355 MHz) and LHC (400 MHz) cavities to save material cost. Besides potential cost savings and additional benefits due to increased stability against thermal breakdown, sputtered films offer the additional advantage of a strongly reduced sensitivity of the residual resistance of sputtered films to DC magnetic fields (0.15nΩ/mOe instead of 0.6nΩ/mOe in Nb). The reduced effect of magnetic field on the residual resistivity was a fortuitous discovery, believed to be related to a higher upper critical field of sputtered niobium (2.5-3.5 T at 4.2 K) due to a larger rate of structural defects and contamination. The most successful coating method to date is based on cylindrical magnetron sputtering, together with chemical etching (or electro-polishing) and thorough rinsing of the copper substrate. The coating is typically 2 µm thick. The Niobium layer grows perpendicularly to the substrate in long rod-like grains. Initial problems with poor film adhesion and contamination were solved in the course of an extensive R&D program. The achieved operating gradients (at the same quality factor), however, are a factor 2-3 lower than in bulk Niobium cavities. 256 cavities of this type have been successfully used in the LEP accelerator at a gradient of 6 MV/m ($Q_0 > 4 \cdot 10^9$), [16]. Today, other approaches for bonding Nb on Cu, such as explosion bonding and co-extrusion, are being pursued for TESLA in combination with novel seamless cavity fabrication techniques such as hydro-forming or spinning.

3.3 Nb_3Sn

Nb_3Sn has been pursued as a potential material for superconducting RF since the mid-seventies. The two times larger T_c of Nb_3Sn with respect to Niobium should result in a smaller surface resistance and higher Q, despite of a larger penetration depth (see Table 2). Forming Nb_3Sn on a Niobium substrate would be an ideal upgrade policy for existing Niobium cavities to higher gradients in the future. The Nb_3Sn cavity development was pursued by the University of Wuppertal, [18,19], CERN, [20], Cornell, [21], TJNAF, [22,23], and SLAC, [24]. Most groups used a Tin vapor solid diffusion process, which consists of exposing the inner surface of a bulk Niobium or sputtered Niobium cavity to a 1100-1200°C Tin and Tin-Chloride vapor followed by a removal of the superficial layer (using oxy-polishing) containing phases which were formed during cool-down with the wrong stoichiometry. Exceptionally high Q's of the order of 10^{11} could be achieved with Nb_3Sn coated cavities. Unfortunately this performance was limited to a modest gradient regime (10-15 MV/m on axis in single-cell prototypes) because of a strong, yet unexplained Q-slope (see Figure 3). Various explanations have been brought forward, among them field dependent surface resistance contributions related to inter-grain weak links, [25], and flux flow resistance after flux penetration, [26]. Another impediment is related to thermo-electric currents at the bi-metal junction at the substrate-superconductor interface, [27]. Apparently special thermal cycling profiles can mitigate this effect, [28]. A serious, remaining issue, which any production process has to address, is the sensitivity of the superconducting Nb_3Sn phase to experimental conditions during formation: the required stoichiometric composition is 18 - 25 atomic % Sn.

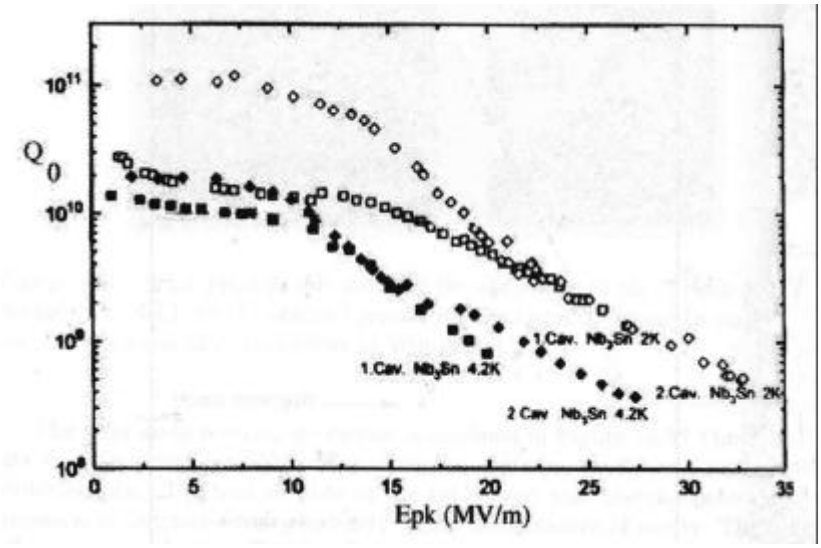

Figure 3: Nb_3Sn cavity tests by TJNAF and Wuppertal, as reported in [36]. Shown are Q measurements at different temperatures (2 K, 4.2 K) for two single-cell, 1.5 GHz, prototypes.

Figure 3 shows, that Nb_3Sn cavities have failed to reach high gradients at high Q. Also, the Nb_3Sn coated cavity prototypes have been plagued by thermal quenching, presumably as a result of a low substrate RRR due to contamination occurring during the coating process. Other possible disadvantages of Nb_3Sn are its low thermal conductivity, the formation of unwanted phases and its brittleness, [17]. Other, less successful techniques used for the preparation of Nb_3Sn cavities were electron-beam co-evaporation, [29], electron-beam evaporation of Sn on a high RRR Nb substrate, [30], and diffusion from Sn layers, [31].

3.4 Other Materials

After, first disappointing results, [32], the Orsay/Karlsruhe collaboration, [33], finally produced 9 GHz TE_{011} cavities and cylindrical rods with sputter coated and thermally diffused NbN films on Niobium. The thermal diffusion film deposition process consisted in heating the Niobium cavity in vacuum to 1850°C, followed by rapid quenching in N_2 atmosphere. The best results obtained on thermally diffused NbN films revealed a factor 3 lower surface resistance than Nb (at 4.2 K). The Saclay group also produced small samples of sputter coated NbTiN and a 7 GHz NbN cavity, [34]. The Genoa University group produced small samples of NbN and NbTiN via N_2 vapor diffusion on a Nb or NbTi-alloy substrate at 1100°C, [35]. The samples were tested at 7.9 GHz, showing promising results. Different diffusion temperatures were explored. They also produced a 3 GHz NbTiN cavity made from a NbTi alloy with this technique, [36,37].

Following the 1987 discovery of high temperature superconductors (HTS), a large number of experiments were carried out to test the RF properties of these new compounds, among them mainly YBCO and BiSCCO. Most of these experiments revealed disappointingly high surface resistance. The ANL-TJNAF group, for example, found a surface resistance in the mΩ range at 4.2 K, 1 GHz and modest RF fields (~10 mT) for their best YBCO samples [38,47]. These results were confirmed by numerous other groups, such as at Wuppertal ([39]-[45]) and Cornell (single crystals –[25]) universities. It is believed that a large penetration depth, inter-grain resistance due to short coherence length, anisotropy and multi-gap structure are the root causes for the high surface resistance found in HTS material up to date, [46]. Material preparation issues certainly played a role as well.

4. Experimental Techniques in RF Material Characterization

4.1 Surface Resistance Measurement at High Power

Many different experimental arrangements were developed to measure the high power microwave properties of superconducting materials, of which the most important is the surface resistance. The by far most popular and successful approach is to fabricate an entire cavity and to measure its quality factor Q. Pulsed schemes using high power klystrons have been devised to measure ultimate quench fields, [48]. The quench criterion typically used was that 90% of the cavity had to be still superconducting, representing a drop in Q of one order of magnitude. Note that this approach yields only an average surface resistance value over the entire cavity surface. Furthermore it is expensive and time consuming. In addition, cavities are often limited by field emission or thermal quenches. This approach also makes it difficult to discriminate between performance limitations related to the superconducting surface itself or damage inflicted during the cavity production.

Therefore, there has always been a strong interest to develop "small sample" techniques. Different approaches have been pursued, yielding mixed results. One, very common approach, uses a host cavity, containing the small sample to be tested (Figure 4). Preferably, the small sample is placed in a high field region, e.g. by laying it into the host cavity (Figure 4-1). Another method, the so-called end replacement method, uses a host cavity with disc-shaped samples welded to one end (Figure 4-2). This method needs large samples at low frequency and it is thus typically made for ~10-40 GHz. A variant of this method, which does not suffer the sample size constraint, uses small samples placed into a high field region within a host cavity using a sapphire (low RF loss and high thermal conductivity) rod (Figure 4-3). In the simplest case (shown in Figure 4) the (host) cavities are operated in a TE_{0mn} (and in particular the TE_{011}) mode to reduce currents across the joints between the cylindrical part and the end-plate. In the TE_{011} mode the currents on the end-plate flow azimuthally, thus parallel to the joint. The magnetic field-lines are radial with the peak field distributed within a ring at half the radius. Problematic is degeneracy with the TM_{111} mode. The degeneracy can be removed by giving the cylindrical cavity a conical shape or with a groove such as in Figure 4-3. Also, experience has shown that geometric imperfections (and parasitic modes) have often resulted in heating on the edges of the sample (or at the joints in the case of the end replacement method).

The measurement of the sample surface resistance is performed indirectly through a Q-perturbation method, in which, the overall Q of the cavity is changed by the different (additional) surface resistance contribution of the sample, [46]. The accuracy of the Q-perturbation method is limited by the "filling factor" of the sample surface with respect to the total cavity surface exposed to RF fields, typically resulting in $\mu\Omega$ resolution, which is unacceptable for state of the art materials, aiming at $n\Omega$ surface resistance. Temperature measurements can be superior to Q-measurements and have therefore been used to improve considerably the sensitivity of the above methods.

All these methods, however, have an intrinsic limitation: Materials with lower surface resistance than the host cavity can usually not be tested. Tricks have been used in the attempt to circumvent this limitation, i.e. operation at higher frequency (i.e. cylindrical 21.5 / 86.5 GHz Cu cavities used by the Wuppertal group), where the BCS surface resistance in the superconductor is larger than the surface resistance of e.g. Copper, [48].

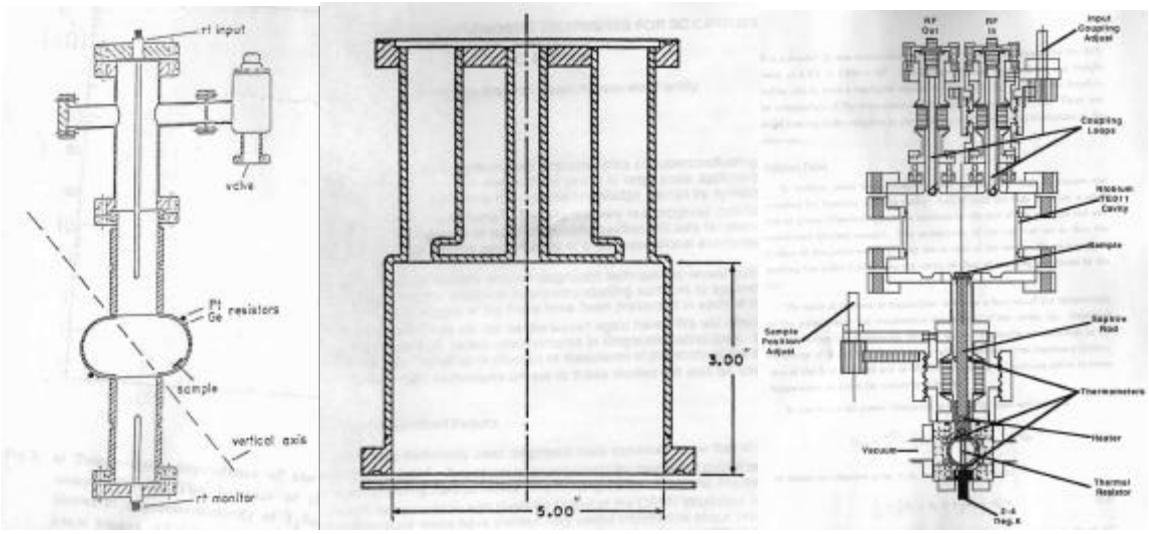

Figure 4: Variations of the sample-in-host-cavity approach: 1) laying sample into host cavity, such as for example in [48], 2) end-replacement TE011 cavity schematic, from [66] and 3) introducing the sample via a sapphire rod as in [46].

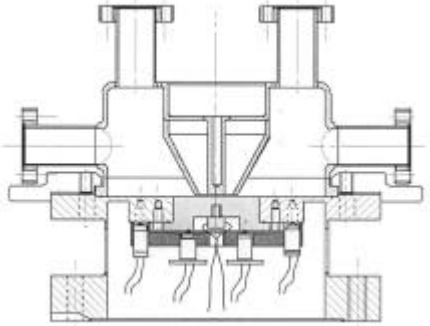

Figure 5: Cern triaxial cavity,[50].

Another approach is to concentrate the fields on the sample. One of the most promising methods pursued so far in this regime is the CERN triaxial cavity operating in a TEM mode at 1.5 GHz, [49,50]. Its design is shown in Figure 5, [51]. The field distribution in the tri-axial cavity is similar to that in a re-entrant cavity, operated in a higher mode. There is a non-zero magnetic field on the cover with a zero-crossing at about 40% of the distance between the central axis and the outer diameter. If the border of the sample coincides with the zero-crossing region there is no RF loss. The surface resistance is measured calorimetrically by thermometers located outside in an evacuated chamber (10μK accuracy). Authors claim a sensitivity of 0.2 nΩ with 25 mT RF field on the sample. The peak fields are limited by the surface resistivity of the Niobium chamber, which was measured to be 2.2 μΩ, attributed to the lack of magnetic shielding, [49]. A disadvantage of the triaxial cavity is the presence of strong electric fields perpendicular to the sample that can result in field emission problems. Another very promising option is the CERN quadrupole cavity, [51]. The quadrupole cavity is essentially a cylindrical resonator with four rods along the cylinder axis that stop short of the end-plate such as to leave a gap for a flat sample. There is a strong azimuthal magnetic field surrounding each rod. The sample is placed on the end-plate, under the rods, in such a way, that it is not in a region of the highest electric field (exactly under the rod) but rather in the region of highest magnetic field (gap between the rods).

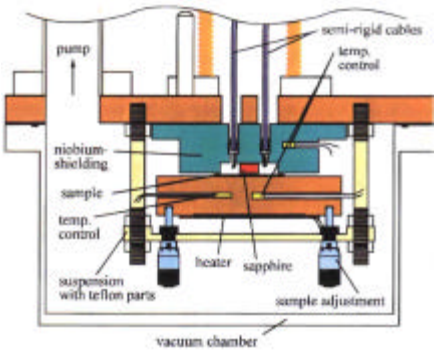

Figure 6: Wuppertal sapphire resonator, [52].

Figure 6 shows the Wuppertal sapphire resonator, [52]. This is a 19 GHz Niobium resonator that uses a 0.5 mm ∅ sapphire rod to enhance fields on the

sample surface, reaching 50 mT with 20 W input power! The limitation of this approach is heating in the sapphire. Frequency can be varied in the range 18-20 GHz via a variation of the gap between sample and sapphire. The Q is derived from the loss in the cavity measured from the difference of incoming and transmitted power, giving a resolution of 20 μΩ (=50 n Ω at 1 GHz).

4.2 Surface Resistance Measurement at Low Power

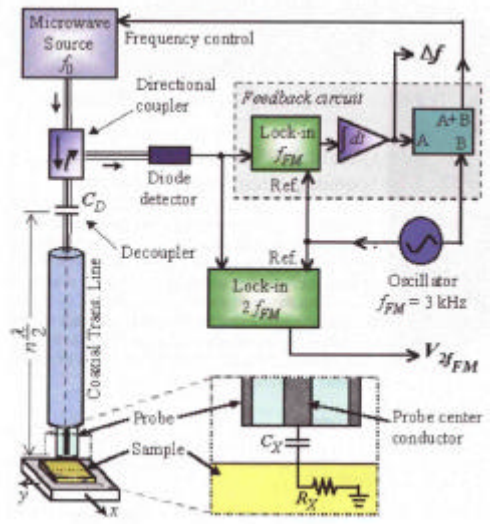

Figure 7: University of Maryland evanescent microwave microscope, [53].

An alternate approach (very similar to the Wuppertal sapphire resonator) is to use low power RF for the measurement of the surface resistance. The University of Maryland, for example, developed an evanescent microwave microscope (Figure 7), which uses 0.1-50 GHz microwave radiation from a (superconducting) co-axial wave-guide to probe a RF surface with ~100 μm resolution, [53]. The coaxial wire with 200 μm inner probe diameter (0.5 mm ∅ coil) couples to the specimen (distance to probe=5μm) yielding a measurement of a Q and a frequency-shift, which is related to the surface resistivity. It is difficult, however, to discriminate between surface topography (as well as un-wanted variations of the probe to surface spacing) and surface resistance. Similar systems have been built as well at the University of Kansas, [54]. The fundamental problem of the low power method is that it does not reveal the "final answer". Furthermore, spatial resolution comes at the price of high (>20 GHz) frequency and the sensitivity of the measurements at low temperature and low surface resistance is not well established. Also, scanning at low temperature is a non-trivial (and yet unaccomplished) task.

4.3 Measurement of the RF Critical Superconductor Parameters

As discussed in chapter 4.1 Yogi et al. proposed critical field measurements driving cavities with high power pulses, [12,55]. This method becomes less accurate as higher field levels are reached (e.g at lower temperature). In the pulsed mode, it is believed, the RF fields can be raised beyond the quench fields of weak spots because the quench propagation time is longer than the pulse duration. When the cavity quenches, it does so due to a global breakdown of the entire cavity surface. As shown in Figure 8, measurements at Cornell using the pulsed method have shown that H_c (the thermodynamic critical field) has been surpassed considerably in Niobium while it has not been reached in Nb_3Sn. Although theory predicts that the superheating critical field, H_{sh}, is smaller than H_c in large κ, type-II superconductors, the quench fields are expected to be much larger than the experimentally achieved.

Besides the cavity based, pulsed measurements there are no other RF critical field measurements for Niobium or Nb_3Sn available. No other experimental technique among

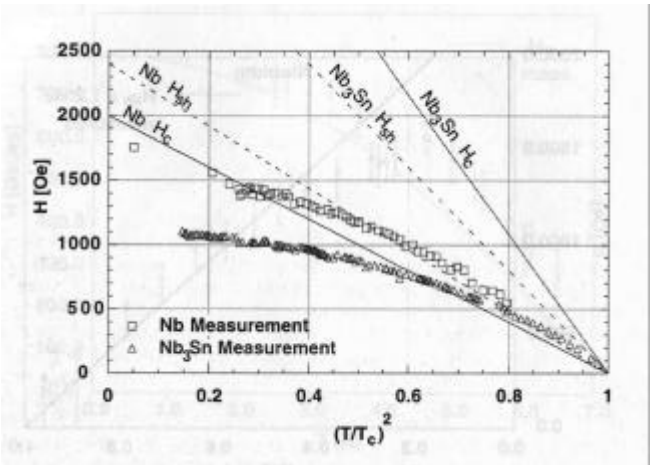

Figure 8: Hays/Padamsee measurement of the quench fields (pulsed mode) in 1.3 GHz bulk Nb cavity and 1.3 GHz / 3 GHz Nb_3Sn/Nb (coated by Sn vapor diffusion on bulk Nb) cavities, [21].

those described in chapter 4.1 has yielded measurements of limiting fields that came close to the expectation shown in Figure 8. Therefore, many laboratories have shifted their emphasis on either low power RF or even DC measurement techniques to characterize the properties of superconductors for RF. The most important are magnetization and DC critical field measurements. DESY with the University of Hamburg perform magnetization measurements with the vibrating magnetometer technique, which consists of moving a DC magnetized (in a 0.5 T background field) sample ($9\times9\times2.8$ mm^3) through an array of pick-up coils. In addition magnetic susceptibility measurements are performed applying alternating (175 Hz) fields to a sample, with pick-up coils that measure the magnetic response of the sample, [13]. Recent measurements using the vibrating magnetometer technique, have revealed an interesting correlation of H_{c3} with Q-slope in sheet Nb samples [56]. The KEK group has developed an apparatus, that measures the voltage induced in a pick-up coil, that is wound around a cylindrical Nb sample in a homogeneous solenoid field, [14]. The inductive voltage response to a slowly ramping magnetic field allows to determine H_{c1} and H_{c2}.

4.4 Surface Analysis and Other Material Property Measurements

It is well known that RF superconductivity takes place in a thin surface layer (the penetration depth of Niobium is 40 nm at 0 K). Surfaces are usually contaminated, irregular and covered with oxides. Therefore surface analysis is an indispensable tool in RF superconductivity R&D. The common surface analysis tools, SEM (scanning electron microscopy), XPS (dispersive X-ray photo electron spectroscopy), AES (Auger electron spectroscopy) can be used not only to determine the surface composition but also, in combination with ablation tools (laser, ion-sputtering) to establish depth profiles (a scrutiny of the results, however, is necessary, as the ablation process may introduce many artifacts). The layer-by-layer surface analysis, however, is tedious and time consuming. It is obvious that the above quoted tools should be part of any superconducting RF materials R&D. As pointed out previously in [57], such tools become especially powerful when combined with small sample RF measurements, allowing to understand the correlation between surface resistance and surface composition. Some laboratories have built integrated, multi-functional surface analysis systems, i.e. the University of Wuppertal system, [58], which includes SEM, AES, FESM (field emission scanning microscope), optical microscope, and a sample preparation chamber. SLAC has an experimental apparatus that includes AES, XPS, EID, SIMS (secondary ion mass spectroscopy) and SEE, [59]. Note that XPS and AES are limited to 1% accuracy. If minute residues of contaminants are to be found, more precise methods are needed, [60]. Other, commonly used measurements in this context are eddy current and SQUID diagnostics of Nb sheets and cavities, [61], flux-gate magnetometry, [62], thermal conductivity and Kapitza resistance measurements, [63],

precision RRR measurements (on grain to grain basis) on Nb sheets using spring loaded needle pins, [64], or via inductive techniques, [65].

5. Proposed research plan

5.1 Outline

This proposal for a superconducting material R&D project is centered around a high power, small sample RF test facility that allows to measure the limiting magnetic field of small RF material samples with fast turn-around and at low cost. As discussed in chapter 4 such a facility would be unprecedented if it could reach surface magnetic fields of ~500 mT and a surface resistance measurement with nΩ resolution. Together with existing surface analysis tools, such as scanning electron microscopy and Auger spectroscopy, this small sample facility could then become a very powerful tool to investigate existing and explore new superconducting RF materials. To support current superconducting RF projects at Fermilab, such as for the CKM project, the small sample test facility could provide measurements on witness samples, that accompany cavity throughout all (or some) production steps. As outlined in chapter 2 the aims of new RF material developments should be cost-reduction and increase of gradient. As a cost savings measure the Nb on copper approach should be pursued. Hot extrusion bonding of Nb and Cu would allow to produce Cu tubes with a thin Nb layer on the inside. These tubes can then be deformed into elliptical cavities using hydro-forming. As discussed in chapter 3 a material with a potential for higher gradients, Nb_3Sn should be explored again. The following gives a discussion of a possible design of such a test facility. It also discusses in further details the material R&D tasks.

5.2 Design of a Small Sample Test Facility

As described in detail in chapter 4 many devices have been invented to allow measuring the limiting RF fields in small samples. None of these techniques, however, achieved 500 mT surface magnetic fields with a nΩ resolution in the surface resistance measurement. These, however, are the basic specifications that a small sample facility should fulfill to allow measurements of for example Nb_3Sn coated samples (assuming that the full potential of this material is realized). It is not obvious that such a small sample facility can be designed and produced. It is certain, however, that the dramatic recent advances in superconducting RF achieved by the TESLA collaboration are now making it possible to achieve a 10-fold increase in maximum fields in a small sample facility of the sample in host cavity type with respect to the last generation of such devices.

We propose to use a state of the art TESLA-type single cell cavity (that is an R&D cavity that has achieved ~200 mT surface fields) in the TE_{010} mode with a small, cylindrical sample being introduced on a rod placed along the center axis of the cavity. Figure 9 shows the electric and magnetic field profiles for the ~2.55 GHz TE_{010} mode in a TESLA 1.3 GHz cavity. The ratio of surface magnetic field on the sample to the cavity surface is ~2. The electric field is torroidal and small on the surfaces of the host cavity. A slight modification of the cavity shape can, in the best case, raise the field enhancement factor to 3.5. The deformation consists mostly in stretching the cavity

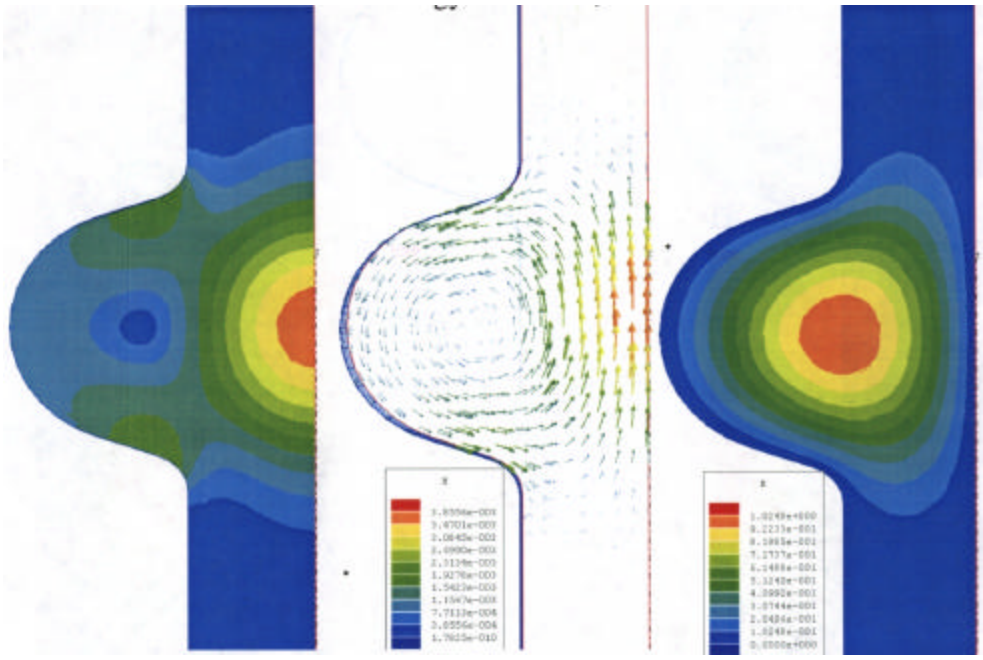

Figure 9: Proposed TE_{010} mode in 1.3 GHz single cell TESLA cavity for short sample facility. Magnetic fields – left and center, electric field – right plot. The magnetic field is highest at the position of the sample. Also, the magnetic field at the sample (center) is parallel to the surface.

along its axis. Calculations indicate the presence of parasitic modes at ~2.48 GHz (TM_{21}) and ~2.61 GHz (TE_{11}). It will require special chokes to damp these modes sufficiently. The design of the coupler is also crucial in this respect. A similar system operating with the TE_{010} mode at 1 GHz would require a ~800 MHz cavity (HERA-type).

Assuming operation at $Q \sim 10^{10}$, a standard function generator and an amplifier unit with a gain of approximately 100 should suffice to supply 100 W of pulsed power to the resonator. The RF pulse height is increased until the sample quenches. If the pulse is to be shorter than 10-100 ms a more powerful power supply system could become necessary. A directional coupler on the input side and a phase-sensitive detector on the output coupler side allow regulation of the power flow. Two parallel measurement methods are proposed to measure the surface resistance, the Q-perturbation and the thermometric methods. The Q perturbation method derives the surface resistance from the change in Q, as inferred from measuring the field attenuation time constant after a pulse, between the reference condition (e.g. no sample, just Nb rod) and the case with the sample. This measurement is performed using a lock-in amplifier to analyze the amplitude ratio of input (from the directional coupler) and output signal (from the phase sensitive detector). The so called filling factor, i.e. the ratio of power dissipation in sample and host cavity is 14% (assuming equal surface resistance in both materials), larger than 5%, the minimum threshold for success of the Q perturbation technique. As discussed in chapter 4 the measurement of the surface quench field can be made more accurate with thermometry. With a resolution of 1 mK, which is less ambitious than the best achieved [66], nΩ surface resistance can theoretically be measured. The calculated dissipation in the sample (host cavity) at 100 mT surface field and 10 nΩ surface resistance is 10 mW / 550 mW, large enough to produce several mK temperature rise in the sample during a 100 msec pulse. For the thermometric method to work, however, it is necessary to insulate the sample thermally from any source of

cooling. The Cernox temperature sensors have to be mounted on the sample holder, such as to be in good thermal contact with the sample and shielded from the RF fields.

Figure 10 shows a schematic of the test-station design. The design is based on the assumption that the host cavity is maintained cold over extensive periods while the samples can be changed without warming the host cavity. This improves turn-around time and prevents contamination of the host cavity. The key part of this design is –1- a low loss cryogenic system that provides a stable 2 K bath to cool the host cavity and –2- a sapphire anti-cryostat, which separates the host cavity vacuum from the sample chamber. The anti-cryostat extends all the way from the room temperature access to the bottom of the host cavity. It needs to be made from sapphire only in the region within the cavity to reduce RF loss. The sapphire walls have to be as thin as possible to reduce the surface electric fields. Note that there might be a need for vacuum on both sides of the sapphire to reduces risk of breakage due to pressure differentials. Also, the OD of the anti-cryostat has to be <25 mm to remain in a region of low enough electric field (<10 MV/m). The electric surface fields on the sapphire have been identified as a major issue in this design and experimental studies will be required to clarify it. The anti-cryostat is cooled in separate stages from room temperature at the top to 2 K within the cavity. There is a LN (~80 K) cooling stage, a ~2 K GHe heat exchanger and a ~2 K conduction cooling stage. The 80 K cooling stage is given by a heat exchanger in series with the cryostat LN shield. The ~2 K heat exchanger stage takes advantage of cold gas pumped from the host cavity bath (it is described in further detail later). The 2 K conduction cooling stage uses large Cu blocks to which the sapphire tube is attached on the top and bottom of the cavity. The copper blocks are cooled by the 2 K host cavity bath. It is necessary to investigate if the low temperature thermal conductivity of sapphire is high enough to rely on conduction cooling only. The sample cooling is provided by an independent cryogenic circuit, described later.

The host cavity is cooled by its own 2 K LHe bath. The 2 K bath is surrounded by a 4.2 K bath to reduce the external heat load. The 4.2 K LHe bath, which can be supplied by a refrigerator or dewars, is not only serving as a thermal shield for the host cavity cavity cryostat, but it is also the reservoir from which helium is pumped to be expanded through a JT valve and cooled to 2 K to supply the host cavity 2 K bath. For this purpose the pressure is lowered on the downstream side of the JT valve, hence in the host cavity bath. (The pumping also reduces the temperature of the cavity bath due to the reduction of the saturated vapor pressure). A heat exchanger system, also shown in Figure 10, is used cool the anti-cryostat (containing the sample) from LN temperature to <4 K with the 2 K gas pumped from the host cavity bath.

The sample holder is essentially a hollow tube that fits into the anti-cryostat. Within the host cavity the sample-holder tube OD must be <20 mm. The sample-holder has to be a hollow tube to allow cooling with helium from within. Assuming a wall-thickness of several mm leaves a ~10 mm cooling duct in the center. The sample has the shape of a ~5 cm long cylinder and is part of the sample holder, such that the sample-holder has a constant OD along its length. The sample is mounted on the sample-holder, such that it is placed in the high magnetic field region in the mid-section of the cavity. The section of the sample-holder that is exposed to RF fields has to be made from high purity Niobium to keep the host cavity Q as high as possible. This is especially true since the operating temperature of the sample-holder can be chosen to be higher than 2 K. The sample-holder, could, for example, consist of a hollow tube with a smaller OD in the lower section. In this way the sample can be slid over the lower section and together with a lower auxiliary cylinder the sample can be held in place and the constant OD condition restored. The sample has to be >5 cm long, so that the edges between the sample and the sample-holder are outside the high magnetic field region.

Edge heating is another major concern in this design. Operation at a higher frequency mode could allow for smaller samples. The sample-holder also has to be centered within the anti-cryostat, preferably without touching it during insertion to protect the sample and Niobium rod surfaces. Furthermore it requires heaters to regulate the temperature of the sample. Also embedded in the sample-holder are temperature sensors to measure the temperature rise in the sample during the quench. The temperature sensor and heater wires run within the sample-holder and are therefore shielded from RF fields. The sample-holder outside the cavity should be made from steel to reduce thermal conduction from the room temperature top to the 2 K bottom.

The sample holder is introduced into the anti-cryostat using the following procedure. A gate valve seals the anti-cryostat vacuum at the top, while the sample is mounted on the sample holder in the preparation chamber (above ground). Ideally the preparation chamber should be under inert atmosphere or somehow protected from airborne contaminants. The sample should be passed into the preparation chamber through a small hatch and mounted using gloves. In order to reduce risk of contamination of the anti-cryostat, the preparation chamber should be evacuated before opening of the gate valve and lowering of the sample into the anti-cryostat. This process should not take more than 1 hour. Once the sample is in place a helium transfer line is connected to the top of the sample-holder and cool-down can begin. The sample-holder also needs to be cooled to 4 K externally, e.g. through conduction from the anti-cryostat in which it

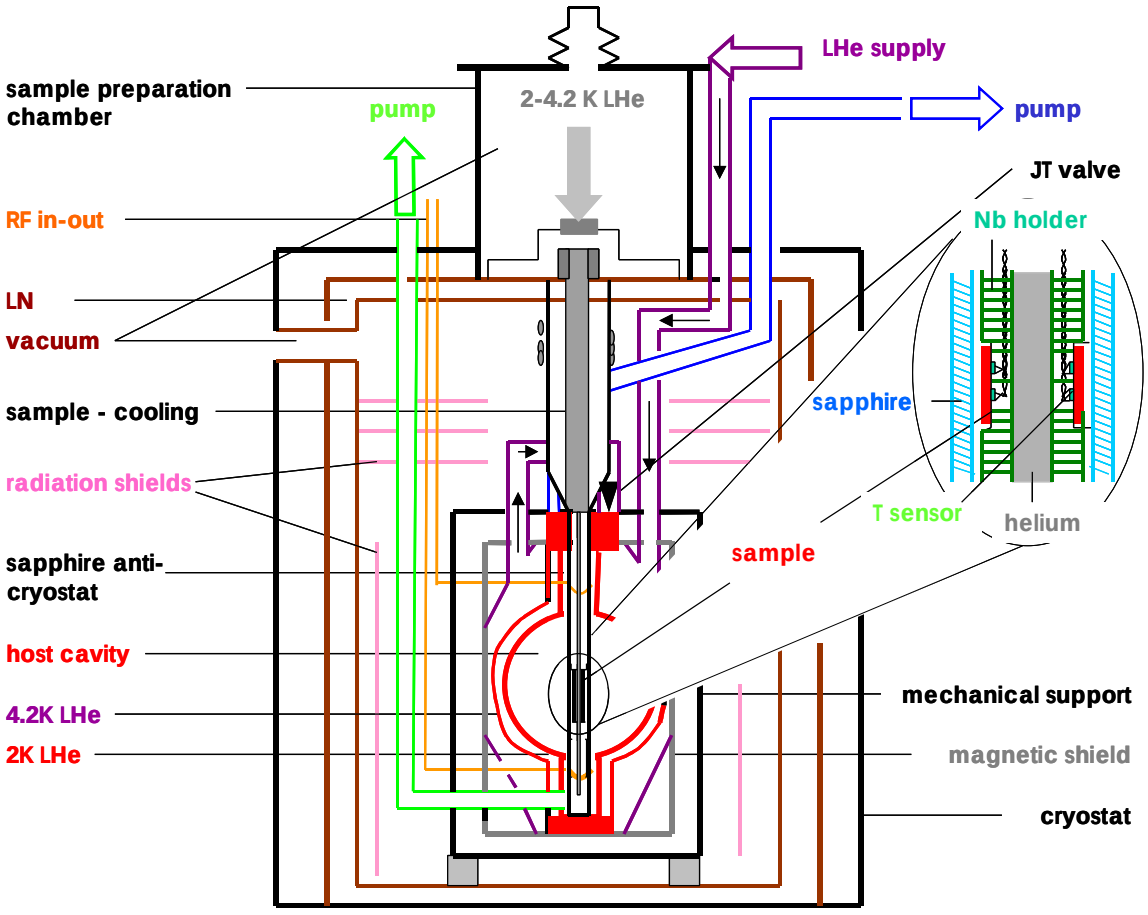

Figure 10: : Sketch of short sample test facility.

runs. Flexible copper blades can be used to establish good thermal contact between the sample-holder tube and the anti-cryostat(which is actively cooled in three stages). As indicated in Figure 10 the sample-holder (and anti-cryostat) should have a larger OD along the top part. This increases the volume of helium in the sample-holder and allows to bring the sample-holder and the anti-cryostat into direct contact (e.g. using flexible copper blades) in their upper section without affecting the lower section that has a smaller OD. The Niobium rod and the sample should never touch anything while being lowered into the host cavity.

Additional hardware required for the sample test-facility consists of various pumping systems to provide the host cavity vacuum, the main dewar vacuum and the sample chamber vacuum. A LN shield is built into the cryostat and also serves to maintain the anti-cryostat at ~80 K underneath the cryostat top-plate (which is at room temperature). Also mechanical support and magnetic shielding have to be provided to the host cavity. The usual diagnostics comprising various LHe meters and temperature sensors as well as pressure gauges will allow control of the test facility parameters. It also has to be noted that the test-facility requires radiation shielding: it presumably will be placed in a pit. The facility does not have to operate in a clean-room environment, if it is kept under vacuum at all time. As outlined above precautions have to be taken to prevent contamination of the sample and anti-cryostat during introduction of the sample into the test facility, [67].

A step-by-step approach is proposed for the development of the facility. In a first stage tests of the host cavity (without sample) should be conducted for example in the A0 cavity test facility. In a second stage tests should be performed in which a Niobium rod is introduced into the host cavity. Then, tests using the sapphire tube around the central rod should be performed. Only if all these benchmark tests are successful, the full implementation of the test-facility should be pursued. Once operational it is imagined that this facility is kept cold continuously, with daily sample exchanges and tests being conducted.

5.3 Materials

As discussed above, the small sample facility can be used as a test-bed for RF material development. As discussed in chapter 2.2 the alternate technology to bulk Niobium with high potential pay-off is bonding of a thin Niobium layer on a Copper substrate. Plating on dissolvable substrates (such as glass) and plasma spraying were tried on small scales in the past. Sputtering, the most successful technology to date, is still being pursued at CERN, but it is not clear whether this technology will further improve to meet the TESLA gradient requirements (see discussion in chapter 3.2). Initial results at KEK, [69], using co-drawing of Niobium and Copper tubes to form the bi-metal (another bonding technique) are promising. A DESY-KEK-TJNAF collaboration has recently reported 40 MV/m on axis gradients in a very successful single cell cavity produced from explosion-bonded Cu/Nb tubes shaped by hydro-forming [70]. Given this extraordinary success, explosion bonding has attracted a lot of attention, since it is suitable for seamless cavity production, allowing to reduce cavity cost significantly, not only through materials cost but more importantly through elimination of expensive welds. One of the interesting aspects of explosion bonding is that a plasma jet is expelled from where the sheets are joint at the head of the pressure wave propagating through the bi-metal interface, cleaning the to be bonded surfaces. Recent samples of explosion bonded Cu-Nb bi-metal tubes, however, have shown cracking and partial de-bonding. Different substrate materials, more similar to Nb in their mechanical

properties, such as Al-alloys could be explored. Issues pertaining to the assembly of an entire accelerator grade cavity have to be addressed also. E.g., how thin can the Nb layer be to utilize standard Nb welding to attach input and HOM couplers. In case of very thin Nb layers the question arises whether bi-metal tubes can also be used in the coupler designs. Therefore, we see a long list of potential R&D issues related to the explosion bonding technique.

Alternatively, a promising variation of this technique, not yet attempted, was recently proposed: hot extrusion, [68]. Hot extrusion is well developed and routinely used in the industrial fabrication of superconducting wire and it promises to produce a smooth copper-niobium interface as well as minimize stress deformation of the external surfaces. The following procedure could be envisaged for the production of superconducting cavities with hot extrusion. Two cleaned, coaxial tubes of Cu and Nb are assembled over a central Cu rod, such that a ~ 0.5 mm Nb layer is surrounded at the inside and outside by Cu. The Nb should be high RRR (~600) grade and in the shape of a tube (and not low RRR sheets such as in the wire fabrication). Seamless tubes can be produced from sheets by spinning. The cleaning of the Cu and Nb tubes can be as sophisticated as required, including high temperature out-gassing and etching. Cu nose and end pieces are attached to the ends of the tube assembly by electron beam welding in vacuum. The entire assembly process takes place in a class 10 clean-room. Prior to extrusion, the assembly can be hot isostatically pressed in order to remove any void space between layers, which may result in distorsion during extrusion. The hot extrusion process, which is currently subcontracted by the superconducting wire manufacturers to Nutech, Canada, consists in pushing the tube assembly through a heated die. Typical extrusion ratios are 4-16, i.e., the diameter is reduced by a factor 2-8, and the length is increased by a factor of 2-4. The hot extrusion step creates clean surfaces, which enhance the diffusion bonding process. The differential thermal contraction between the Cu and Nb leaves the Nb in compression and prevents the Nb from cracking or tearing during subsequent forming steps. Nitric acid and/or machining can be used to remove the copper rod from the inside. BCP-type etching can follow to obtain a clean and smooth Nb surface on the inside of the so-formed hollow tube. Such a tube can then be hydroformed into a cavity We propose to test the hot extrusion technology on small samples before proceeding to cavity production. The small samples can be in the form of hollow tubes, with the outer Cu shell removed to leave the active surface (Nb) on the outside.

Similarly as in the case of Nb coating a study is required to define the most promising technology for the deposition of Nb_3Sn on Nb or preferably Nb/Cu cavities. Although the tin-vapor solid-diffusion process has been found to be the most successful route in the past (see discussion in chapter 3.3), other alternate techniques should be studied also. Among them could be electro-plating followed by laser heating. The small sample test facility would be an ideal tool to study different coating technologies with fast turn around. Also, a possible expansion of the program to include NbN should be considered.

5.4 Task List and Preliminary Budget for 03

Table 3 summarizes the project goals, Table 4 summarizes the major budget items and Table 5 summarizes the human resources required for the remainder of 2003 in the frame of the superconducting RF material R&D project.

Table 3: FY03 goals – superconducting RF materials R&D.

Goal	Description
1	model test of single cell TESLA cavity with central Nb-rod
2	test of single cell TESLA cavity with central Nb-rod
3	test of single cell TESLA cavity with central sapphire
4	design of small sample test facility
5	nurture and extend collaborations with universities and other laboratories

Table 4: Budget proposal for FY03 - superconducting RF material R&D.

	comment	k$
RF test equipment	RF source, coupler, DAQ electronics	10
TESLA one-cell R&D cavity	DESY	10
Sapphire tube	single crystal	10
Miscellaneous parts for cavity test	flanges, welding for rod assembly	5
Materials for small samples	raw materials (Nb, Cu,.), first samples	5
External Analysis of small samples	e.g. Auger spectroscopy, first trials	5
Helium for testing	BOC dewars	5

Table 5: Human resources requirements for FY03 - superconducting RF materials R&D.

Type	Task(s)	Duration
Technician	prepare cavity&rod test	2 months
Designer	design of small sample facility	6 months
RF Engineer/Physicist	rod in cavity test and design of small sample facility	2 months
Cryo-Engineer	test station cryo-system design	4 months
Instrumentation Eng,	instrumentation for small sample test facility	2 months
Materials-Scientist	develop procedures for small sample preparation and start production of samples (e.g. Nb rod, small Nb samples) and start surface analysis activity in collaboration with external institutions	Half-time
Physicist - I	manage program, direct small sample test facility design and initial testing and procurement	Full-time

Given the challenge that the small sample test station represents, the FY03 will essentially be spent for its conceptualization and design. The most important goal is certainly to prove the feasibility of the small sample test idea presented above in the form of the rod in cavity test. Also important is the preparation of lab-space and the continued collaboration with the university partners.

References

[1] M. McAshan, R. Wanzenberg", "RF Design of a Transverse Mode Cavity for Kaon Separation", Fermilab Note TM-2144, May 2001

[2] G.W. Foster, "8 GeV Linac Concept", Fermilab, Beams Division Seminar, Jan. 14th 2002, http://tdserver1.fnal.gov/project/8GevLinac/

[3] Linear Collider R&D list as found at http://www-conf.slac.stanford.edu/lcprojectlist/projectlist/intro.htm

[4] W.M. Fairbank, J.M. Pierce, P.B. Wilson, Proceedings of the 8th Conference on Low Temperature Physics, Butterworth, p. 324, Washington 1963

[5] I.E. Campisi, Z.D. Farkas, “The Pulsed RF Superconductivity Program at SLAC”, SLAC-PUB-3412, Aug. 1984
[6] TESLA Design Report, DESY-2001-11, March 2001
[7] H. Safa, “High Field Behavior of SCRF Cavities”, Proceedings of the 10th workshop on RF superconductivity”, 2001
[8] P.H. Garbincius, H. Edwards, “Report on the TESLA Engineering Study / Review”, Fermilab TM-2179, July 2002
[9] W. Singer, “Niob fuer TESLA”, TESLA-Report 2001-27
[10] W. Weingarten, “Superconducting Cavities – Basics”, CAS 95 Proceedings, CERN96-03
[11] W.D. Moeller, Proceedings of the 7th Workshop on RF Superconductivity in Saclay, France, 1995
[12] T. Yogi, G.J. Dick, J. E. Mercereau, “Critical RF fields for some type-I and type-II superconductors”, Physical Review Letters, Vol. 39/13, p. 826, Sept. 1977
[13] M. Bahte, F. Hermann, P. Schmueser, “Magnetization and Susceptibility Measurements on Niobium Samples for Cavity Production”, Proceedings of the 8th workshop on RF superconductivity, 1997
[14] K. Saito, talk at FNAL Nb workshop in May 2002, htttp://www-bd.fnal.gov/niobium
[15] J. Halbritter, “On RF Residual Losses in Superconducting Cavities”, Proceedings of the 2nd Workshop on RF Superconductivity”, Cern 1984
[16] E. Chiaveri, p. 200 of the Proceedings of the 1996 EPAC, S. Myers, editor, IOPP Publishing, Bristol
[17] B. Hillenbrand, “The Preparation of Superconducting Nb3Sn Surfaces for RF applications”, Proceedings of the first Workshop on RF Superconductivity, KFK, Karlsruhe, July 1980
[18] H. Heinrichs et al., “Activities on RF-Superconductivity at Wuppertal”, Proceedings of the 2nd RF superconductivity workshop, Part-2, CERN 1984
[19] M. Peininger et al., “Work on Nb3Sn Cavities at Wuppertal”, Proceedings of the 3rd RF superconductivity workshop at ANL, ANL-PHYS-1, p. 503, Argonne, 1987
[20] G. Arnolds-Mayer, E. Chiaveri, “On a 500 MHz Single Cell Cavity with Nb3Sn Surface”, Proceedings of the 3rd RF superconductivity workshop ANL 1988, ANL-PHYS-1, 1988, p. 491
[21] H. Padamsee, T. Hays, “Measuring the RF critical fields of Pb, Nb and Nb3Sn”, Proceedings of the 8th RF superconductivity workshop 1997, p. 794
[22] P. Boccard, P. Kneisel, G. Mueller, J. Pouryamount, H. Piel, “Results from some temperature mapping experiments on Nb3Sn RF cavities”, JLAB-ACT-98-02
[23] Roeth, Kneisel, Proceedings of the 7th RF superconductivity workshop , Saclay 95
[24] I.E. Campisi, “On the Limiting RF fields in Superconducting Accelerator Cavities”, Technical Report, SLAC/AP-58, 1987
[25] H. Padamsee, J. Knobloch, T. Hays, “RF Superconductivity for Accelerators”, J. Wiley & Sons, 1998, p.319
[26] W. Weingarten, “Progress in Thin Film Techniques, Particle Accelerators Vol 53, No 1-4, Proceedings of the 7th Workshop on RF Superconductivity, Saclay Oct. 1995
[27] P. Boccard, P. Kneisel, G. Mueller, J. Pouryamount, H. Piel, “Results from some temperature mapping experiments on Nb3Sn RF cavities”, JLAB-ACT-98-02
[28] Personal communication – S. Calatroni, CERN
[29] L.H. Allen, M.R. Beasley, R.H. Hammond, J.P. Turneaure, IEEE Trans. Mag., MAG-19, p. 1003, 1983
[30] H. Padamsee, “Superconducting RF Activities at Cornell University”, Proceedings of the 3rd Workshop on RF Superconductivity, ANL-PHYS-1, Argonne, 1987
[31] J. Hasse , W. Hermann, R. Orlich, Zeitschrift fuer Physik 271, p. 265, 1974
[32] V.N. Tuong et al., “RF Superconductivity at Orsay”, Proceedings of the 2nd RF superconductivity workshop, Part 2, CERN 1984
[33] M. Pham Tu, K. Mbaye, L. Wartski, J. Halbritter, “Niobium Nitride Coated Superconducting Cavities”, Proceedings of the 3rd RF superconductivity workshop, ANL 1988, ANL-PHY-88-1
[34] S. Cantacuzene, PhD thesis, “Elaboration et Characterisation de couches minces de NbTi pour des applications en hyperfrequences”, Uni Paris-Sud/Orsay, 1995

[35] G. Gemme, P. Fabricatore, R. Musenich, R. Parodi, M. Viviani, B. Zhang, "RF Surface Resistance Measurements of Binary and Ternary Niobium Compounds", Journal of Applied Physics, 77, 1995, p.257
[36] A. Dacca, G. Gemme, R. Musenich, R. Parodi, S. Pittaluga, S. Rizzini, V. Buscaglia, "Niobium Titanium Nitride for Superconducting Accelerating Cavities", Proceedings of the 8th RF superconductivity workshop 1997, p. 1103
[37] "Study of Nb-Nitrides for SC RF cavities", P. Fabbricatore, INFN-FM-89-1, 1989
[38] J.R. Delayen, C. L. Bohn, C. T. Roche, "Measurements of the Surface Resistance of High Tc Superconductors at High RF fields", in Journal of Superconductivity, Vol. 3, No. 3, p. 243, 1990
[39] H. Padamsee, J. Knobloch, T. Hays, "RF Superconductivity for Accelerators", J. Wiley & Sons, 1998, p.315
[40] T. Hays, H. Padamsee, "Measuring the RF Critical Field of Pb, Nb and Nb3Sn", Proceedings of the 8th RF superconductivity workshop 1997, p. 789
[41] N. Klein, p. 285 of the Proceedings of the 5th Workshop on RF Superconductivity, D. Proch, editor, DESY – M-92-01
[42] M. Hein, p. 267 of the Proceedings of the 7th Workshop on RF Superconductivity, B. Bonin, editor, CEA/Saclay 9608011, 1995
[43] G. Mueller, p. 267 of the Proceedings of the 4th Workshop on RF Superconductivity, Y. Kojima, editor, KEK 1990
[44] G. Mueller, p. 2085 of the Proceedings of the 1996 EPAC, S. Myers, editor, IOPP Publishing, Bristol
[45] H. Piel et al., "Experiments on the RF Surface Resistance of the Perovskite Superconductors at 3 GHz", Proceedings of the 3rd RF superconductivity workshop, ANL, 1988, ANL-PHYS-1, p. 197
[46] D.L. Rubin et al,. "RF Measurements on High Tc Materials", Proceedings of the 3rd RF Superconductivity workshop, ANL, 1988, ANL-PHYS-1, p.211
[47] C. Liang, p. 307 of the Proceedings of the 6th Workshop on RF Superconductivity, R.M. Sundelin, editor, CEBAF, 1994
[48] H. Piel, "Superconducting Cavities 1+2" in CAS 88 Proceedings – CERN-89-04
[49] C. Liang, L. Phillips, R. Sundelin, "A New Method of Surface Resistance Measurement with a Niobium Triaxial Cavity Working at 2 K", Rev. Sci. Instrum,. 64 (7), p. 1937, July 1993
[50] E. Mahner, W. Weingarten, "A feasibility study of a triaxial cavity to determine the surface resistance of superconducting samples", Proceedings of the 8th RF superconductivity workshop, 1997, LNL-INFN (Rep) 133/98, p. 316
[51] E. Mahner, "A New Instrument to Measure the Surface Resistance of Superconducting Samples at 400 MHz", CERN Divisional Report CERN AT/2003-1 (VAC), April 2003, to be published in Review of Scientific Instrumentation
[52] T. Kaiser, W. Diete, M. Getta, M.A. Hein, G. Mueller, M. Perpeet, H. Piel, "Niobium Shielded Sapphire Resonator for Field Dependent Surface Resistance Measurements of Superconducting Films", Proceedings of the 8th RF superconductivity workshop, 1997, LNL-INFN (Rep) 133/98
[53] S. Anlage, C.P. Vlahacos, D. E. Steinhauser, S. K. Dutta, B. J. Feenstra, A. Thanawalla, F.C. Wellstood – "Low Power Superconducting Microwave Applications and Microwave Microsopy", Proceedings of the 8th RF superconductivity workshop, 1997, LNL-INFN (Rep) 133/98
[54] S. E. Babcock et al., "Electrical Connectivity and Microstructure in YBa2Cu3O7-Films on Rolling-Assisted Biaxially-Textured Substrates", Proceedings of International Congress on Intergranular and Interphase Boundaries (iib'98) in Materials Science Forum, p 165, 1999
[55] T. Yogi, "Radio Frequency Studies of Surface Resistance and Critical Magnetic Field of Type I and Type II Superconductors", PhD thesis, CalTech, 1977
[56] B. Steffen U Wuerzburg/DESY, recent measurements of Hc3 in sheet Nb samples, personal communication, March 2003
[57] A. Septier, "Surface Studies and Electron Emissions", Proceedings of the 1st Workshop on RF Superconductivity, KfK Karlsruhe, July 1980

[58] N. Pupeter et al., "Influence of Surface Roughness and Preparation, Bulk Purity and Heat Treatment on Electron Field Emission from Nb and Nb3Sn", Proceedings of the 7th workshop on RF superconductivity, Saclay, France, 1995, p.67
[59] E.L. Garwin, R. Kirby, Surface Studies of Nb, its Compounds, and Coatings", SLAC-PUB-3378, July 1984
[60] C. Antoine, "Surface Studies – Method of Analysis and Results", Proceedings of the 7th workshop on RF superconductivity, Saclay, France, 1995, p. 647
[61] W. Singer, D. Proch, "Diagnostics of Defects in High Purity Niobium", Proceedings of the 8th RF superconductivity workshop 1997, p. 850
[62] V. Palmieri, F. Stivanello, M. Valentino, "Flux-Gate Magnetometry: The Possibility to Apply A Novel Tool to Monitor Niobium Chemistry", Proceedings of the 9th RF superconductivity workshop, 1999
[63] S. Bousson, M. Fouaidy, T. Junquera, N. Hammoudi, J.C. LeScornet, J. Lesrel, "Kapitza Conductance and Thermal Conductivity of Materials used for SRF Cavities Fabrication", Proceedings of the 9th workshop on RF superconductivity, 1999
[64] H. Safa, M. Bolore, Y. Boudigou, S. Jaidane, R. Keller, P. Nardin, G. Szegedi, "Specific Resistance Measurements of a Single Grain Boundary in Pure Niobium", Proceedings of the 9th workshop on RF superconductivity, 1999
[65] H. Safa, Y. Boudigou, E. Jacques, J. Klein, S. Jaidane, M. Bolore, "Inductive RRR Measurements ..", Proceedings of the 8th workshop on RF superconductivity, 1997, p.864
[66] C.E. Reece, "Progress in Diagnostic Techniques for SC Cavities", Proceedings of the 3rd workshop on RF Superconductivity, ANL, ANL-PHYS-88-1, p. 545, 1987
[67] P. Kneisel, "Clean Work and its Consequences", Proceedings of the 2nd Workshop on RF Superconductivity, Cern 1984
[68] R. Scanlan, "New Fabrication Approaches for Superconducting RF Cavities", draft of proposal, Jan. 4th 2002
[69] K. Saito, personal communication, Nov 2002
[70] W. Singer et al., Proceedings of the 10th Workshop on RF Superconductivity, KEK 2000

Appendix A

The number of accelerating structures (including the overhead factor *OH*) drops linearly with gradient, such that the total linac cost, (1), runs through a broad maximum, diverging at very low gradient due to the large number of structures and at very high gradient due to the high cost per structure. The calculation below assumes a slope factor *k* of \$ 1.9 k/(MV), an overhead factor, *OH*, of 1.2 and an offset C_{cav0} of \$ 5 k/m for the linear rise of the cavity cost with gradient.

$$C_{linac}(G) = \frac{E_{com}(MeV)OH}{G\left(\frac{MV}{m}\right)}\left[C_{cav0} + kG\left(\frac{MV}{m}\right)\right] \quad (\$) \qquad (1)$$

The cryo-power operations cost, (2) is calculated from the cryo-power per unit length, the total linac length and the cost factor c in (\$/W/year). The cryo-operations cost, for a acceleration voltage, rises linearly with gradient. The cryo-power per unit length is calculated from the loss in the cavity walls, the duty factor, the Carnot factor for (T_b=) 2 K operation f_C (see (3)), a fiddle factor *FF* (accounting for the fact that the wall power loss is typically only a fraction of the total dynamic RF loss in the cavity) and the static cryo-load, p_{stat}.

$$C_{cryo} = \left[\frac{G^2}{2R_s} \frac{1}{f_C(T_b)} t_{pulse} f_{rep} FF + p_{stat} \right] \frac{E_{com} OH}{G} N_{year} c\left(\frac{\$}{W - year} \right) \ (\$) \qquad (2)$$

wall-loss power incl. Carnot | duty-factor | static power | length of linac | power cost factor

(3) is the Carnot factor for a 30% efficiency cryo-plant. The Carnot factor at 2 K is 497.

$$f_C(T_b) = 0.3 \frac{T_b}{300K - T_b} \qquad (3)$$

The tunneling infrastructure cost is calculated from the linac length and the tunneling cost per unit length ($ 9 M/km).

Appendix B

The quality factor Q is given in (4) as a function of the cavity shunt impedance, R_{shunt}, and the material dependent surface resistance, R_s, here given in terms of a semi-phenomenological, experimental fit. The surface resistance depends on the residual surface resistance R_0, the frequency (here 1.3 GHz), the bath temperature T_b and the gap parameter a (a=17.7 K for Nb and 39.6 K for Nb_3Sn). Figure 2 shows the calculated Q for Nb and Nb_3Sn with two possible residual surface resistances (2 and 10 nΩ).

$$Q(T_b) = \frac{R_{shunt}}{R_s(T_b)} \qquad R_s(T_b) = R_0 + \frac{9 \cdot 10^{-5}}{T_b} f(GHz)^2 e^{-\frac{a}{T_b}} \quad (\Omega) \qquad (4)$$